NIH Public Access
Author Manuscript
Cancer Prev Res (Phila). Author manuscript; available in PMC 2012 June 1.

Published in final edited form as:
Cancer Prev Res (Phila). 2011 June ; 4(6): 879–889. doi:10.1158/1940-6207.CAPR-11-0025.

Targeting p53 Null Neuroblastomas through RLIP76**

Jyotsana Singhal, **Sushma Yadav**, **Lokesh Dalasanur Nagaprashantha**, **Rit Vatsyayan**, **Sharad S Singhal***, and **Sanjay Awasthi***
Department of Molecular Biology and Immunology, University of North Texas Health Science Center, Fort worth, TX 76107

Abstract

The search for p53-independent mechanism of cancer cell killing is highly relevant to pediatric neuroblastomas, where successful therapy is limited by its transformation into p53 mutant and a highly drug-resistant neoplasm. Our studies on the drug-resistant p53 mutant as compared with drug-resistant p53 wild-type neuroblastoma revealed a novel mechanism for resistance to apoptosis: a direct role of p53 in regulating the cellular concentration of pro-apoptotic alkenals by functioning as a specific and saturable allosteric inhibitor of the alkenal-glutathione-conjugate transporter, RLIP76. The RLIP76-p53 complex was demonstrated both using immuno-precipitation analyses of purified proteins as well as by immuno-fluorescence analysis. Drug transport studies revealed that p53 inhibited both basal and PKCα stimulated transport of glutathione-conjugates of 4HNE (GS-HNE) and cisplatin. Drug resistance was significantly greater for p53 mutant as compared with p53 wild-type neuroblastoma cell lines, but both were susceptible to depletion of RLIP76 by antisense alone. In addition, inhibition of RLIP76 significantly enhanced the cytotoxicity of cisplatin. Taken together, these studies provide powerful evidence for a novel mechanism for drug and apoptosis resistance in p53 mutant neuroblastoma, based on a model of regulation of p53 induced apoptosis by RLIP76, where p53 is a saturable and specific allosteric inhibitor of RLIP76, and p53 loss results in over-expression of RLIP76; thus, in the absence of p53, the drug and glutathione-conjugate transport activities of RLIP76 are enhanced. Most importantly, our findings strongly indicate RLIP76 as a novel target for therapy of drug-resistant and p53 mutant neuroblastoma.

Keywords

RLIP76; p53; Neuroblastoma, Glutathione-conjugates transport; xenografts; drug-resistance

Introduction

Neuroblastomas are the most common solid tumors in infants and represent the third most common class of pediatric malignancies (1). Neuroblastomas arise from the neural crest tissue of the sympathetic ganglia. Neuroblastomas can metastasize to the liver where the metastatic tumors can be massive (2). The most common metastatic site is the skull where it metastasizes to sphenoid bone and retro bulbar tissue leading to common symptoms of proptosis and periorbital echymosis (3,4). Surgical resection of localized neuroblastomas offers good clinical remission but advanced stages of neuroblastomas require aggressive

**This work was supported in part by USPHS grant CA 77495 (SA & SS), the Cancer Research Foundation of North Texas (SS & SY) and Institute for Cancer Research & the Joe & Jessie Crump Fund for Medical Education (SS).

***Address correspondence to:** Sanjay Awasthi, M.D., Professor, or Sharad Singhal, Associate Professor, University of North Texas Health Science Center, Fort Worth, TX 76107-2699; Phone: 817-735-0459; Fax: 817-735-2118; sanjay.awasthi@unthsc.edu or sharad.singhal@unthsc.edu.

NIH-PA Author Manuscript
NIH-PA Author Manuscript
NIH-PA Author Manuscript

NIH-PA Author Manuscript

NIH-PA Author Manuscript

NIH-PA Author Manuscript

multi-modality treatment (1,5,6). The other treatment modalities currently being investigated in refractory and relapsed neuroblastomas include anti-angiogenic drugs and fenretinide, a retinoid derivative (7,8). Given the limited three year event free survival of 15% in the incident population and the nature of symptoms in affected children, validation of novel drug targets becomes a vital focus of translational research in order to achieve complete therapeutic response in multi-drug resistant neuroblastomas (9-11).

The tumor suppressor p53 plays a significant role in multi-drug resistance of neuroblastomas. Though the p53 mutations are relatively rare in primary neuroblastomas, advanced neuroblastomas acquire loss-of-function mutations in p53 which render them resistant to conventional chemotherapeutic regimens (12-14). It is an established fact that p53 mediates the induction of apoptosis in cells treated with chemotherapeutic drugs and loss-of-function mutations in p53 are associated with resistance to both anti-cancer drugs and radiation therapy (15,16). The use of chemotherapeutic drugs like cisplatin (CDDP), doxorubicin (DOX) and vincristine is highly limited in refractory and relapsed neuroblastomas due to frequent loss-of-function mutations in the tumor suppressor p53 (17,18).

The human ral-binding protein 1(RALBP1 or RLIP76) is a 76 kDa multi-functional drug transport protein with substrate stimulated ATPase-activity and over-expressed in majority of cancers like cancers of the lung, colon, kidney, melanoma, ovary, prostate and breast (19,20). Normally, RLIP76 functions as an anti-apoptotic and stress protective protein that prevents accumulation of oxidative-stress induced toxic metabolites inside the cells. RLIP76 acts by catalyzing the ATP-dependent efflux of glutathione-electrophile conjugates (GS-E) of lipid peroxidation products (19). In the previous studies, we have shown that the inhibition of RLIP76 by antisense induced selective apoptosis in several cell lines of lung, prostate, kidney, colon, and breast cancers (19,20). The hallmark of inhibition of RLIP76 in our previous tumor models of various cancers has been selective toxicity towards targeted tumor cells sparing normal cells.

Until today, the investigations into the mechanisms of p53-induced apoptosis in neuroblastoma have been focused on the inhibition of cell cycle checkpoints upon DNA-damage and induction of the transcription of apoptotic proteins like bax, bak and PUMA upon cytotoxic stimuli to cells (21). The non-nuclear and transcription independent mechanisms of p53-mediated cell death include stimulation of caspase3 activation by mitochondrial translocation of p53 upon exposure to radiation (22). In the current study, we investigated the interaction of p53 on the multi-drug transporter RLIP76 followed by the analysis of the impact of RLIP76 inhibition in targeting multi-drug resistant neuroblastoma. We used two p53wild-type (SMS-KCNR and LAN-5) and two p53-mutant (CHLA-90 and SKN-BE2) neuroblastoma cell lines for our studies. CHLA-90 is a neuroblastoma cell line derived at progressive stage of neuroblastoma following multi-agent chemotherapy and SKN-BE2 is derived from recurrent neuroblastoma. Neuroblastomas established as cell lines following acquisition of drug-resistance during multi-drug therapy and maintained without exposure to drugs during regular cultures still retain the properties of specific drug-resistance that was acquired during initial multi-drug chemotherapy (23). Thus, the neuroblastoma cell lines with mutant p53 were relevant to specifically study the loss-of-p53 induced drug-resistance in neuroblastoma.

Materials and Methods

Reagents

Doxorubicin was obtained from Adria Laboratories (Columbus, OH). Cisplatin was obtained from Bristol-Meyers Squibb (Princeton, NJ). Source of polyclonal rabbit anti-human rec-

NIH-PA Author Manuscript

NIH-PA Author Manuscript

NIH-PA Author Manuscript

RLIP76 antibodies was same as previously described (24). P53 antibodies were purchase from Santa Cruz, CA. Maxfect transfection reagent was from MoleculA (Columbia, MD). PKCα was obtained from Molecular Probes, Oregon. 4HNE and MDA measurements kit was purchased from Oxis International, Beverly Hills, CA. Gene-specific primers, scrambled as well as RLIP76-antisense were purchased from Biosynthesis Inc. (Lewisville, TX). Radio-labeled ^{3}H-GSHNE (specific activity 3.1×10^{4} cpm/nmol) was synthesized as described by us previously (25). ^{14}C-DOX (specific activity 54 mci/mmol) was purchased from Amersham Corporation (Arlington Heights, IL).

Cell Lines

CHLA-90 and SKN-BE(2) (p53 mutant) cell lines have been established from tumors obtained from patients who had relapsed after intensive multi-agent myeloablative chemo-radiotherapy and bone-marrow transplantation. SMS-KCNR and LAN-5 (p53 wild-type) cell lines have been established from tumors obtained from neuroblastoma patients. Human neuroblastoma cell lines were kindly authenticated and provided in May 2010 by Dr. Patrick Reynolds, M.D., Ph.D., Children's Neuroblastoma Cancer Foundation / Children Oncology group, Texas Tech University, Department of Cell Biology & Biochemistry, School of Medicine, Lubbock, TX. The cells were tested for *Mycoplasma* once at the beginning immediately after receiving the cell lines and after 3 months. All the experiments were performed within five months of securing the cell lines. Cells were grown in complete medium consisting of Iscove's modified Dulbecco's medium supplemented with 3 mM L-glutamine, insulin and transferrin 5 μg/ml each, 5 ng/ml of selenous acid (ITS culture supplement) and 20% FBS at 37 °C in a humidified 5% CO_2 atmosphere. Cell lines were sub-cultured by detaching without trypsin from culture plates using a modified Puck's Solution A plus EDTA (Puck's EDTA) which contain 140 mM NaCl, 5 mM KCl, 5.5 mM glucose, 4 mM $NaHCO_3$, 0.8 mM EDTA, 13 μM phenol red, and 9 mM HEPES buffer, pH 7.3.

Cross-linking and immuno-precipitation

The protein-protein cross-linking and immuno-precipitation assay was performed according to the method of Aumais et al (26). Briefly, purified rec-RLIP76, and p53 (10 μg each) were cross-linked by incubation with 0.1 mM N-succinimidyl 3-(2-pyridyldithio) propionate (SPDP; from Sigma) in a total volume of 0.5 ml in 10 mM sodium phosphate buffer, pH 7.4, for 30 min. Excess SPDP was removed by passing the solution through a Sephadex G-50 spin column pre-equilibrated with sodium phosphate buffer (pH 7.4). The samples were treated with 0.5 mM N-ethylmaleimide for 10 min to block all free SH groups that could prematurely cleave cross-links. Protein complexes were immune-precipitated by incubating with either pre-immune IgG or anti-RLIP76 IgG for 12 h followed by with protein A-Sepharose (20 μl of 50% bead slurry) in radio-immuno-precipitation assay buffer (50 mM Tris-HCl, pH 7.4, 4 mM EDTA, 150 mM NaCl, 1% Triton X-100 and 0.1% SDS) for 2 h. Samples were sedimented by centrifugation at 10,000 × g, washed three times with radio-immuno-precipitation assay buffer, and then resuspended in 100 μl of SDS-PAGE sample buffer. To check the effect of PKCα in the interaction of RLIP76-p53, the immuno-precipitation was performed in the presence of equimolar concentration of PKCα in the absence and presence of 1 mM ATP. The reaction mixture was incubated for 30 min at 37 °C and the cross-linking and immuno-precipitation was performed as described above. Samples were analyzed by SDS-PAGE and Western-blotting against anti-RLIP76, anti-PKCα and anti-p53 IgG.

NIH-PA Author Manuscript

NIH-PA Author Manuscript

NIH-PA Author Manuscript

4HNE and MDA Levels

Measurement of endogenous levels of 4HNE and MDA in a panel of neuroblastoma cells were performed spectrophotometrically by using the LPO 586 (Oxis International, Beverly Hills, CA) measurement kit according to Manufacturer's instructions.

Drug-sensitivity assay

Cell density measurements were done using a hemacytometer to count dye-excluding cells resistant to staining with trypan blue. Approximately 2×10^4 cells were plated into each well of a 96-well flat-bottomed micro-titer plate 24 h prior to addition of medium containing varying concentrations of antibodies or drugs. After 24 h incubation, 40 μl aliquots of drugs (DOX and CDDP) diluted in medium were added to get final concentration between 0.001 μM and 100 μM to 8 replicate wells. After 96 h incubation, 20 μl (5mg/ml stock) MTT was added to each well and incubated for 2 h at 37 °C. The plates were centrifuged and medium was removed. Formazan dye trapped in cells was dissolved by addition of 100 μl DMSO with gentle shaking for 2 h at room temperature, followed by measurement of absorbance at 570 nm. Depletion of RLIP76 expression in cells by RLIP76-antisense was measured as follows: cells were incubated for 6 h with 0-10 μg/mL RLIP76-antisense in Maxfect transfection reagent (Molecula A) according to the manufacturer provided protocol.

Liposome preparation

The proteoliposome preparation procedures used here have been validated and described in detail previously (24,27). Briefly, proteoliposomes containing RLIP76 or p53 were prepared by addition of the purified recombinant protein to a sonicated emulsion of 1:4 cholesterol and phospholipids (soybean asolectin, 95% purity, Sigma Chemicals Co) in liposome reconstitution buffer (10 mM Tris-HCl, pH 7.4, 2 mM $MgCl_2$, 1 mM EGTA, 100 mM KCl, 40 mM sucrose, 2.8 mM BME, 0.05 mM BHT, and 0.025% polidocanol). Liposome formation was initiated by addition of SM2 Biobeads (200 mg/mL). We have shown that vesiculation is complete within 4 h and yields primarily unilammelar vesicles with median diameter of 0.25 μm and intra-vesicular / extra-vesicular volume ratio of 18 μL/mL (24). The control liposomes or the liposomes reconstituted with purified RLIP76 were used for transfecting cells in culture. Efficiency of delivery for RLIP76-proteoliposomes has been established previously (24).

Radiation-protection by RLIP76-liposomal delivery

2.5×10^3 CHLA-90 and SMS-KCNR cells were treated with control-liposome and RLIP76-proteoliposomes (50 μg/mL final conc.) for 24 h prior to radiation at 100 to 500 cGY using a Varian Clinac linear accelerator (2100 C; 6-MeV photon beams) at the Texas Cancer Center, Arlington, TX. Cells were inoculated into colony-forming assays immediately after radiation. After 7 days, colonies were stained with methylene blue and counted using an image acquisition and analysis system (Innotech Alpha Imager HP). The results presented are the mean and s.d. from three separate experiments. Please note that CHLA-90 (6255 colonies/ml); and SMS-KCNR (6620 colonies/ml); plating efficiency of CHLA-90 and SMS-KCNR are 1 and 1.06, respectively. After RLIP76-proteoliposomes treatment; CHLA-90 (6255 to 7130 colonies/ml); and SMS-KCNR (6620 to 7035 colonies/ml); plating efficiency of CHLA-90 and SMS-KCNR after RLIP76-proteoliposomes treatment are 1.14 and 1.06, respectively.

Preparation of total crude fractions for Western-blot analyses

Cells were pelleted and washed with balanced salt solution. Washed cells were lysed and sonicated for 30 seconds at 50 W and incubated for 4 h at 4 °C with occasional shaking. After incubation, the resultant preparation was centrifuged at 105,000 × g for 60 min at 4

NIH-PA Author Manuscript

NIH-PA Author Manuscript

NIH-PA Author Manuscript

°C. The supernatant was collected and aliquots of crude-fraction were applied to SDS-PAGE and Western-blot analyses were performed. Western-blots were developed by enhanced chemiluminescence reagent (Pierce).

Immuno-cytochemistry for interaction of RLIP76 and p53

Co-localization of RLIP76 and p53 was performed on neuroblastoma, LAN-5 (wild-type p53) and SKN-BE2 (mutant p53) fixed cells by method described previously with slight modifications (28). Briefly, cells were grown on glass cover-slips and fixed with methanol and acetic acid (3:1). Nonspecific antibody interactions were minimized by pretreating the cells with 10% goat serum in TBS for 60 min at room temperature. The cells were subjected to immuno-cytochemistry using anti-RLIP76 IgG (raised in rabbit) and anti-p53 IgG (raised in mice) as a primary antibody and goat-anti-rabbit rhodamine red-x-conjugated (for RLIP76) or goat-anti-mouse FITC-conjugated (for p53) as secondary antibody. DAPI (4′, 6-Diamidino-2-phenylindole) was used as a nuclear counter-stain. Slides were analyzed by confocal laser microscope (Leica TCS-SP5, Germany).

Depletion or inhibition of RLIP76-expression by RLIP76-antisense and antibody

Depletion of RLIP76-expression by RLIP76-antisense (2-10 μg/mL) was done using Maxfect Transfection Reagent according to manufacturer's protocol. Briefly, cells were incubated for 6 h with 2-10 μg/mL RLIP76-antisense, washed with PBS, followed by 48 h incubation at 37 °C in medium. For inhibition of RLIP76, anti-RLIP76 IgG at a concentration of 10 - 20 μg/mL was used.

Transport of ^{14}C-DOX and ^{3}H-GSHNE by RLIP76 and its inhibition by p53

For these experiments, fixed amount of purified rec-RLIP76 (250 ng) was reconstituted into proteoliposomes along with varying amounts (0-250 ng) of purified rec-p53, in the absence/presence of 12.5 ng of PKCα, 1 mM ATP, and were incubated for 30 min at 37 °C. Effect of PKCα-mediated phosphorylation on RLIP76-mediated ^{14}C-DOX and ^{3}H-GSHNE transports were measured as described (27,29). In one control p53 proteins were excluded while in other control equivalent amount of BSA were reconstituted in proteoliposomes. Each determination was performed in triplicate.

Animal model

Hsd: Athymic nude nu/nu mice were obtained from Harlan, Indianapolis, IN. All animal experiments were carried out in accordance with a protocol approved by the Institutional Animal Care and Use Committee (IACUC). Twenty 11-weeks-old male mice were divided into four groups of 5 animals (treated with pre-immune serum, scrambled anti-sense DNA, anti-RLIP76 IgG, and RLIP76 antisense). All 20 animals were injected with 2×10^6 Neuroblastoma cells (SMS-KCNR) suspensions in 100 μL of PBS, subcutaneously into one flank of each nu/nu nude mouse. Animals were examined daily for signs of tumor growth. Treatment was administered when the tumor surface area exceeded 40 mm^2 (~28 days). Treatment consisted of 200 μg of anti-RLIP76 IgG or antisense in 100 μL PBS, i.p. Control groups were treated with 200 μg/100 μL pre-immune serum or scrambled antisense-DNA. Tumors were measured in two dimensions using calipers.

Statistical analyses

All experiments were performed in triplicates. The experimental data was statistically analyzed by two-tailed unpaired student's t test or by one way ANOVA and are expressed as the mean + SD. A value of $p < 0.05$ was considered statistically significant.

NIH-PA Author Manuscript

NIH-PA Author Manuscript

NIH-PA Author Manuscript

Results

Multi-drug resistance and expression of RLIP76 in p53-mutant Neuroblastomas

We first compared the neuroblastoma cells expressing wild-type p53 and mutant p53 for multi-drug resistance upon treatment with chemotherapeutic, drugs DOX and CDDP. The CHLA-90 and SKN-BE2 cells with mutant p53 were more resistant for all the tested drugs than the SMS-KCNR and LAN-5 cells with wild-type p53. The IC_{50} values for DOX were 0.60 ± 0.1 μM and 0.88 ± 0.1 μM in CHLA-90 and SKN-BE2 p53 mutant cells, respectively, which were significantly higher by an order of magnitude of ~35 fold when compared to p53 wild-type neuroblastomas (IC_{50}: 0.02 ± 0.0 μM). The IC_{50} values for CDDP were 30 ± 4 μM and 22 ± 2 μM in CHLA-90 and SKN-BE2 p53 mutant cells, respectively, which were significantly higher by order of magnitude of 3-7 fold when compared to p53 wild-type neuroblastomas (IC_{50}: 4 ± 1 μM and 10 ± 1 in SMS-KCNR and LAN-5 cells, respectively) (Table 1). P53 is one of the key regulators of anti-oxidant network of the cells and the interplay between reactive-oxygen-species (ROS) and p53 is complex (30). Wild-type p53 in response to stress and DNA-damage in normal cells activates pro-oxidant genes leading to increased ROS and apoptosis of damaged cells. Wild-type p53 in non-stressed cells stimulates the transcription of anti-oxidant genes leading to reduced ROS and thus protects the ROS-induced mutations in genes (30). Thus, the neuroblastoma cells with mutant p53 in regular cultures should possibly differ in the oxidative-stress. The level of end-products of lipid peroxidation of 4-hydroxynonenal (4HNE) and malondialdehyde (MDA) were substantially higher in p53 mutant neuroblastoma cells compared to wild-type p53 expressing neuroblastoma cells (Fig 1A; $p < 0.001$). But, interestingly, the p53 mutant neuroblastomas with higher and toxic oxidative-stress markers like 4HNE and MDA were resistant to apoptosis induction by chemotherapy drugs relative to neuroblastomas with wild-type p53. Thus, in addition to lack of p53 function in multi-drug resistant neuroblastomas, it indicated a possibility for up-regulation of cellular defense against toxic end-products of ROS. Hence, we studied the expression of RLIP76, a multi-specific transporter of GS-E of lipid peroxidation and chemotherapy drugs. We observed that the expression of RLIP76 was significantly higher in p53 mutant as compared to p53 wild-type neuroblastomas (Fig 1B). These findings indicate that the p53 mutant neuroblastomas might be dependent on the function of RLIP76 to buffer the enhanced oxidative-stress. RLIP76 regulates the cellular concentration of products of lipid-peroxidation. 4HNE, a marker of oxidative-stress, has concentration dependent effects in cells. Moderate levels of 4HNE stimulate proliferation whereas very high levels of 4HNE are toxic to even transformed and relatively apoptosis-resistant cancer cells (31). We observed that p53 mutant neuroblastoma cells have higher levels of 4HNE in spite of higher expression of the GS-HNE transporter RLIP76. This could be attributed to activation of cyp2E1, in p53 mutant neuroblastomas, which enhances the generation of 4HNE from ω-6 fatty acids (32,33). Thus, p53 mutant neuroblastomas have higher 4HNE relative to p53 wild-type cells, but they may not be able to reach very toxic concentrations due to RLIP76 over-expression. Thus, the “moderately high levels of 4HNE” attained due to a fine calibration between cyp2E1 mediated enhanced generation of 4HNE and RLIP76 mediated efflux could have stimulatory effect on cellular proliferative pathways.

To further confirm the protective effects of RLIP76 in neuroblastomas, we supplemented one p53 mutant (CHLA-90) and one p53 wild-type (SMS-KCNR) neuroblastoma cells with RLIP76 by liposomal delivery and tested the radiation-sensitivity in relation to respective cell lines transfected with control-liposomes. RLIP76 delivery protected both the cell lines from toxic oxidative-stress induced upon radiation-exposure (Fig 1C).

NIH-PA Author Manuscript

NIH-PA Author Manuscript

NIH-PA Author Manuscript

Immuno-precipitation and Immuno-cytochemistry analysis of the interaction of RLIP76 with p53

As RLIP76 was increased in p53 mutant neuroblastoma cell lines, we next investigated the functional status of RLIP76 in the presence or absence of p53. In this regard, we first analyzed whether p53 interacts with RLIP76 or not in the presence of equimolar-concentrations of RLIP76 and PKCα, a known activator of RLIP76. Our previous studies have indicated that PKCα phosphorylates RLIP76 on S^{118}, T^{297}, S^{353} and S^{509} (29). Hence, we wanted to study whether the PKCα-mediated phosphorylations have any impact on the binding-assay. Immuno-precipitation studies revealed that RLIP76 binds with p53 both in the presence and absence of PKCα and that any phosphorylation by PKCα is not essential for the binding of p53 to RLIP76. But, the binding of p53 to RLIP76 was enhanced in the presence of PKCα and ATP (F**ig 2A**, **Lane 5**). Next, we analyzed the binding of p53 to RLIP76 in SKN-BE2 cells expressing mutant p53 and LAN-5 cells expressing wild-type p53. Immuno-cytochemistry for the binding of RLIP76 and p53 revealed enhanced p53 binding to RLIP76 in LAN-5 neuroblastoma cells relative to p53 mutant SKN-BE2 cells as revealed by an yellow overlay fluorescence when stained with fluorescent antibodies for RLIP76 (red, rhodamine) and p53 (green, FITC) (Fig 2B). Thus, the confirmation of enhanced binding of wild-type 53 over mutant p53 to RLIP76 further lead to investigation of the effect of p53 binding on RLIP76 transport function.

Effect of transfection of p53 on RLIP76-mediated transport of glutathione-conjugates of 4HNE and DOX

The effect of p53 on the transport function of RLIP76 was analyzed in reconstituted liposomes treated with increasing concentrations of p53. P53 caused a concentration dependent decrease in the transport activity of RLIP76. Both the transport of glutathione-conjugates of 4HNE (GS-HNE) and DOX was decreased in the presence of p53 (Fig 3A and B). In the immuno-precipitation studies, we noted an enhanced binding of p53 to RLIP76 in the presence of PKCα (Fig 2A). Hence, we further analyzed the impact of PKCα on p53-mediated inhibition of RLIP76 drug-transport. Co-treatment with PKCα significantly enhanced the p53-induced inhibition of RLIP76-mediated drug-transport in liposomes. In accordance with previously published studies, PKCα in the presence of 1mM ATP activated the drug-transport by RLIP76. P53 caused significant decline in both the basal and PKCα stimulated transport function of RLIP76 (Fig 3C). Also, p53 caused maximum inhibition of RLIP76 transport in the absence of PKCα, but not in the presence of PKCα. Thus, though PKCα stimulates the binding of p53 to RLIP76; functionally, it partially reverses the p53-induced inhibition of RLIP76 transport. Thus, PKCα and p53 have opposite effects on the function of RLIP76 with either of them being able to partially reverse the effect of other. This is significant because previous studies by others have established that malignant neuroblastoma cells express a high level of PKCα along with nMyc and treatment with retinoic acid which induces maturation of neuroblastoma cells to normal neuronal phenotype causes a decline of PKCα levels (34). Thus, the loss-of p53 tilts the balance towards enhanced multi-drug resistance that is mediated by RLIP76 both due to over-expression of RLIP76 as well as uninhibited stimulation of drug-transport by RLIP76 by activators like PKCα in advanced neuroblastomas.

RLIP76 inhibition induces cell-death and enhances CDDP-sensitivity in neuroblastoma

We further investigated the effect of inhibition of RLIP76 using antibodies and antisense. Depletion of RLIP76 by antisense increased the cell-death in neuroblastoma cells (Fig 4A). RLIP76 inhibition substantially enhanced the sensitivity to CDDP in both p53 mutant neuroblastoma cell lines along with those expressing wild-type p53 (Fig 4B; $p < 0.01$). The marginally enhanced susceptibility of p53 wild-type SMS-KCNR and LAN-5 neuroblastoma cells to RLIP76 antisense induced cell death and potentiation of CDDP toxicity may be due

NIH-PA Author Manuscript

NIH-PA Author Manuscript

NIH-PA Author Manuscript

to the activation of alternate p53 dependent apoptotic pathways consequent to RLIP76 depletion induced oxidative stress and enhanced intracellular drug concentrations in a p53 wild-type background. But, the substantial cell death in p53 mutant neuroblastoma cell lines reflects the ability of RLIP76 depletion alone to induce cell death which, along with the RLIP76 inhibition induced increase in drug sensitivity in p53 null background, is of specific relevance in the control of aggressive and drug resistant p53 null neuroblastomas.

RLIP76 inhibition alone causes tumor-regression in mice xenografts of Neuroblastoma

The novel finding that RLIP76 depletion alone using antisense was effective in targeting neuroblastomas lead to further investigations. Both the p53 mutant CHLA-90 and SKN-BE2 cell lines did not form tumors in mice xenografts. Hence, we tested the impact of RLIP76 inhibition on mice xenografts of SMS-KCNR cells. 2×10^6 neuroblastoma cells were injected in 100 μL PBS into subcutaneous flank of each nu/nu mice and tumors were allowed to develop. At ~ day30, when the tumors reached approximately 40 mm^2 the mice were treated with 200 μg of RLIP76 antibodies or antisense in 100 μL of PBS and tumor-growth was observed everyday by measuring the tumor cross sectional area using calipers. The RLIP76 inhibition alone, either by using antibody or antisense caused significant tumor-regression (Fig 5A). The average weight of tumors of treated mice was substantially lower than the controls (tumor weight at day 44: Control-1.88g, RLIP76-antibody or antisense treated −0.39 g; Fig 5B and C; $p < 0.001$). There was no loss in the weight of treated mice when compared to controls which ruled out any dose limiting overt off-target cytotoxicity consequent to RLIP76 inhibition. This confirmed the ability of RLIP76 inhibition to successfully induce neuroblastoma tumor-regression. Though, p53 mutant neuroblastomas did not develop tumors in mice-xenograft studies, the significant efficacy of RLIP76 inhibition or depletion in p53 normal neuroblastoma was a striking finding for the ability to target RLIP76 alone in neuroblastomas. Taken together, our mice-xenograft studies in p53 normal neuroblastomas along with the preceding drug-transport studies where p53 inhibits RLIP76 and cell survival studies where RLIP76 is effective to a greater extent in p53 mutant neuroblastoma cell lines, the current research findings provide strong mechanistic and biological rationale for targeting RLIP76 in both p53 normal and p53 mutant neuroblastomas to achieve effective therapeutic response.

Discussion

Neuroblastomas are the most aggressive form of neuroblastic tumors with ganglio-neuroblastoma and ganglio-neuroma being the other succeeding aggressive tumors originating from the neural crest cells. Neuroblastomas have a median age of onset at 23 months and cause approximately 15% of the total cancer deaths in pediatric population. The neuroblastomas diagnosed before 18 months have good prognosis and many cases show spontaneous regression even without any clinical interventions. But, the survival of neuroblastomas incident after 18 months of age is poor at 42% (35). The neuroblastomas that occur in adolescents represent immense challenge to current interventions and are highly fatal (36). Approximately 60% of neuroblastomas present with metastases at different organs like liver, bone-marrow and cortical bones at the time of presentation which limits localized surgical approaches and necessitates aggressive and effective chemotherapeutic interventions to achieve complete cure (37). Thus, targeting drug-resistant and relapsed tumors represents a contemporary focus of management in neuroblastomas.

Amplification of nMyc is an established cause in primary neuroblastomas, but nMyc is positively associated with aggressive course of disease in children greater than 1 year at the time of diagnosis but not in infants (38-40). Treatment of neuroblastoma cells with cyclophosphamide induces apoptotic response by activating p53 dependent transcription of apoptotic genes like PUMA and activation of pro-apoptotic proteins bax, bim, caspase 3 and

NIH-PA Author Manuscript

NIH-PA Author Manuscript

NIH-PA Author Manuscript

caspase 9. P53 mediated apoptotic pathway is frequently altered in multi-drug resistant and relapsed neuroblastomas due to several causative factors (41). The nMyc amplication leads to attenuation of p53 function by stimulating the over-expression of p53 inhibitor Mdm2 (42).

Loss-of-function mutations in p53 lead to over-expression and uninhibited action of RLIP76 which contributes to chemo-resistance. The p53 mutant neuroblastomas have enhanced levels of oxidative stress as revealed by increased concentration of 4HNE and MDA. Previous studies from our laboratory have demonstrated that increased oxidative-stress stimulates the expression of RLIP76 in K562 cells (43). Thus, p53 mutant neuroblastomas could be activating the transcription of RLIP76 as a stress-responsive protein to defend against toxic effects of enhanced oxidative-stress. It is also possible that p53 could have a direct transcriptional role in regulating the expression of RLIP76. In this regard, the exact mechanisms that contribute to over-expression of RLIP76 in p53 mutant neuroblastomas need to be investigated further.

In addition to enhancing the chemosensitivity of co-administered drugs like CDDP, RLIP76 alone represents as a highly significant therapeutic target in multi-drug resistant neuroblastomas. Inhibition of RLIP76 alone induced significant cell-death which was more pronounced in p53 mutant neuroblastomas. Over-expression of RLIP76 in p53 mutant cancers it self could be a major pathogenetic factor for aggressive and metastatic neuroblastomas. In addition to its fundamental role in efflux of GS-E of lipid peroxidation products and chemotherapy drugs, RLIP76 regulates a spectrum of signaling events in cancer cells that are of importance in proliferation and metastases (Fig 6). CDK1 binds to RLIP76 and translocates it to nucleus where it mediates the separation of chromosomal spindles during mitosis (44). PKCα-mediated proliferation and drug-resistance require RLIP76 (29). RLIP76, through its RhoGAP domain, directly binds to and mediates adhesion dependent activation of the GTPase R-Ras leading to enhanced cell motility that was mediated by downstream Rac-activation (45). RLIP76 is also negatively regulated by previously known inhibitors like HSF-1, POB-1 and CDC2 (46,47). P53, as evident from our current studies, is a novel inhibitor and arguably the most significant inhibitor in the context of multi-drug resistance associated with loss-of-p53 in multiple malignancies. Most importantly, RLIP76 inhibition in our previous tumor models of mice did not reveal any deficits in the CNS functions and the experimental mice were active and normal without any loss of weight (48-50).

In summary, RLIP76 is a potential target for therapeutic interventions in refractory and relapsed neuroblastomas. In addition to well defined nuclear and mitochondrial mechanisms of initiating p53 mediated apoptosis, for the first time, our results have established a novel “cell membrane” mechanism where active p53 inhibits the multi-drug transporter RLIP76 to initiate a cascade of cell-death events that are mediated by an increase in intracellular concentration of ROS to toxic levels along with enhancing the intracellular concentration of administered chemotherapy drugs. The observed absence of off-target cytotoxicity as evident from our previous studies in RLIP76-targeted mice further corroborates the relevance of RLIP76 targeted chemotherapy for pediatric neuroblastomas as such intervention would not compromise the normal growth and development of treated children. Thus, RLIP76 represents a novel and effective therapeutic target to treat multi-drug resistant neuroblastomas.

Acknowledgments

The authors thank Dr. Xiangle Sun, core facility at the University of North Texas Health Science Center, Fort Worth, TX, for helping with flow cytometry and laser capture micro-dissection (supported by NIH Grant ISIORR018999-01A1). We also thank Dr. Sumihiro Suzuki, Department of Biostatistics, School of Public Health,

University of North Texas Health Science Center, Fort Worth, TX, for his assistance in the statistical analyses of the data.

The abbreviations used are

RLIP76	ral-binding protein, Ralbp1
DOX	doxorubicin
GSH	glutathione
GS-E	glutathione-electrophile conjugate
4HNE	4-hydroxynonenal
GSHNE	glutathione-conjugate of 4-HNE
CIS	cisplatin
PUMA	p53 up-regulated mediator of apoptosis
R508	RLIP76-antisense phosphorothioate deoxy-oligonucleotide

References

1. Berthold F, Hero B. Neuroblastoma: current drug therapy recommendations as part of the total treatment approach. Drugs. 2000; 59:1261–77. [PubMed: 10882162]
2. Jacob ES, Varghese RG, Toi PC, Bhaskaran R, Rai R. Congenital neuroblastoma with liver metastasis presenting with Hashimoto Pritzker disease. Ind J Pathol Microbiol. 2009; 52:374–6.
3. DuBois SG, Kalika Y, Lukens JN, et al. Metastatic sites in stage IV and IVS neuroblastoma correlate with age, tumor biology, and survival. J Pediatr Hematol Oncol. 1999; 21:181–9. [PubMed: 10363850]
4. Smith SJ, Diehl N, Leavitt JA, Mohney BG. Incidence of pediatric Horner syndrome and the risk of neuroblastoma: a population-based study. Arch. Ophthalmol. 2010; 128:324–29. [PubMed: 20212203]
5. Wei JS, Greer BT, Westermann F, et al. Prediction of clinical outcome using gene expression profiling and artificial neural networks for patients with neuroblastoma. Cancer Res. 2004; 64:6883–91. [PubMed: 15466177]
6. Hawkes WC, Alkan Z. Regulation of redox signaling by selenoproteins. Biol Trace Elem. Res. 2010; 134:235–51. [PubMed: 20306235]
7. Children's Oncology Group (CCG 09709). Villablanca JG, Krailo MD, et al. Phase I trial of oral fenretinide in children with high-risk solid tumors: a report from the Children's Oncology Group (CCG 09709). J Clin. Oncol. 2006; 24:3423–30. [PubMed: 16849757]
8. Garaventa A, Luksch R, Lo Piccolo MS, et al. Phase I trial and pharmacokinetics of fenretinide in children with neuroblastoma. Clin Cancer Res. 2003; 9:2032–39. [PubMed: 12796365]
9. Fong A, Park JR. High-risk neuroblastoma: A therapy in evolution. Pediatr Hematol Oncol. 2009; 26:539–48. [PubMed: 19954363]
10. Kubota M, Okuyama N, Hirayama Y, Asami K, Ogawa A, Watanabe A. Mortality and morbidity of patients with neuroblastoma who survived for more than 10 years after treatment--Niigata Tumor Board Study. J Pediatr Surg. 2010; 45:673–77. [PubMed: 20385269]
11. Modak S, Cheung NK. Neuroblastoma: Therapeutic strategies for a clinical enigma. Cancer Treat Rev. 2010; 36:307–17. [PubMed: 20227189]
12. Seeger RC, Reynolds CP. Treatment of high-risk solid tumors of childhood with intensive therapy and autologous bone marrow transplantation. Pediatr Clin North Am. 1991; 38:393–424. [PubMed: 2006084]
13. Manhani R, Cristofani LM, Odone Filho V, Bendit I. Concomitant p53 mutation and MYCN amplification in neuroblastoma. Med Pediatr Oncol. 1997; 29:206–7. [PubMed: 9212845]

NIH-PA Author Manuscript NIH-PA Author Manuscript NIH-PA Author Manuscript

NIH-PA Author Manuscript

NIH-PA Author Manuscript

NIH-PA Author Manuscript

14. Keshelava N, Zuo JJ, Chen P, et al. Loss of p53 function confers high-level multidrug resistance in neuroblastoma cell lines. Cancer Res. 2001; 61:6185–93. [PubMed: 11507071]
15. Houldsworth J, Xiao H, Murty VV, et al. Human male germ cell tumor resistance to cisplatin is linked to TP53 gene mutation. Oncogene. 1998; 16:2345–9. [PubMed: 9620551]
16. Lee JM, Bernstein A. P53 mutations increase resistance to ionizing radiation. Proc Natl Acad Sci U S A. 1993; 90:5742–6. [PubMed: 8516323]
17. Amaral JD, Xavier JM, Steer CJ, Rodrigues CM. The role of p53 in apoptosis. Discov Med. 2010; 45:145–52. [PubMed: 20193641]
18. Keshelava N, Zuo JJ, Waidyaratne NS, Triche TJ, Reynolds CP. P53 mutations and loss of P53 function confer multidrug resistance in neuroblastoma. Med Pediatr Oncol. 2000; 35:563–8. [PubMed: 11107118]
19. Awasthi S, Singhal SS, Sharma R, Zimniak P, Awasthi YC. Transport of glutathione-conjugates and chemotherapeutic drugs by RLIP76 (RALBP1): a novel link between G-protein and tyrosine kinase signaling and drug resistance. Int J cancer. 2003; 106:635–46. [PubMed: 12866021]
20. Vatsyayan R, Lelsani P, Awasthi S, Singhal SS. RLIP76: A versatile transporter and an emerging target for cancer therapy. Biochem Pharmacol. 2010; 79:1699–705. [PubMed: 20097178]
21. Chesler L, Goldenberg DD, Collins R, et al. Chemotherapy-induced apoptosis in a transgenic model of neuroblastoma proceeds through p53 induction. Neoplasia. 2008; 10:1268–74. [PubMed: 18953436]
22. Erster S, Mihara M, Kim RH, Petrenko O, Moll UM. mitochondrial p53 translocation triggers a rapid first wave of cell death in response to DNA damage that can precede p53 target gene activation. Mol Cell Biol. 2004; 24:6728–41. [PubMed: 15254240]
23. Keshelava N, Seeger RC, Groshen S, Reynolds CP. Drug resistance patterns of human neuroblastoma cell lines derived from patients at different phases of therapy. Cancer Res. 1998; 58:5396–405. [PubMed: 9850071]
24. Awasthi S, Cheng J, Singhal SS, et al. Novel function of human RLIP76: ATP-dependent transport of glutathione-conjugates and doxorubicin. Biochemistry. 2000; 39:9327–34. [PubMed: 10924126]
25. Sharma R, Singhal SS, Cheng J, et al. RLIP76 is the major ATP-dependent transporter of glutathione-conjugates and doxorubicin in human erythrocytes. Arch Biochem Biophys. 2001; 391:171–9. [PubMed: 11437348]
26. Aumais JP, Lee HS, Lin R, White JH. Selective interaction of hsp90 with an estrogen receptor ligand-binding domain containing a point mutation. J Biol Chem. 1997; 272:12229–35. [PubMed: 9115298]
27. Awasthi S, Singhal SS, Pikula S, et al. ATP-dependent human erythrocyte glutathione-conjugate transporter. II. functional reconstitution of transport activity. Biochemistry. 1998; 37:5239–48. [PubMed: 9548755]
28. Yadav S, Singhal SS, Singhal J, et al. Identification of membrane-anchoring domains of RLIP76 using deletion mutant analyses. Biochemistry. 2004; 43:16243–53. [PubMed: 15610018]
29. Singhal SS, Yadav S, Singhal J, Drake K, Awasthi YC, Awasthi S. The Role of PKCα and RLIP76 in Transport-mediated Doxorubicin-resistance in Lung Cancer. FEBS Lett. 2005; 579:4635–41. [PubMed: 16087181]
30. Bensaad K, Vousden KH. Savior and slayer: The two faces of p53. Nat Med. 2005; 11:1278–9. [PubMed: 16333263]
31. Dwivedi S, Sharma A, Patrick B, Sharma R, Awasthi YC. Role of 4-hydroxynonenal and its metabolites in signaling. Redox Rep. 2007; 12:4–10. [PubMed: 17263900]
32. Lee YS, Wan J, Kim BJ, Bae MA, Song BJ. Ubiquitin-dependent degradation of p53 protein despite phosphorylation at its N terminus by acetaminophen. J Pharmacol Exp Ther. 2006; 317:202, 8. [PubMed: 16330492]
33. Bardag-Gorce F, French BA, Nan L, et al. CYP2E1 induced by ethanol causes oxidative stress, proteasome inhibition and cytokeratin aggresome (mallory body-like) formation. Exp Mol Pathol. 2006; 81:191–201. [PubMed: 17034788]

NIH-PA Author Manuscript

NIH-PA Author Manuscript

NIH-PA Author Manuscript

34. Tonini GP, Parodi MT, Di Martino D, Varesio L. Expression of protein kinase C-alpha (PKC-alpha) and MYCN mRNAs in human neuroblastoma cells and modulation during morphological differentiation induced by retinoic acid. FEBS Lett. 1991; 280:221–4. [PubMed: 2013316]
35. London WB, Castleberry RP, Matthay KK, et al. Evidence for an age cutoff greater than 365 days for neuroblastoma risk group stratification in the children's oncology group. J Clin Oncol. 2005; 23:6459–65. [PubMed: 16116153]
36. Franks LM, Bollen A, Seeger RC, Stram DO, Matthay KK. Neuroblastoma in adults and adolescents: An indolent course with poor survival. Cancer. 1997; 79:2028–35. [PubMed: 9149032]
37. DuBois SG, Kalika Y, Lukens JN, et al. Metastatic sites in stage IV and IVS neuroblastoma correlate with age, tumor biology, and survival. J Pediatr Hematol Oncol. 1999; 21:181–9. [PubMed: 10363850]
38. Weiss WA, Aldape K, Mohapatra G, Feuerstein BG, Bishop JM. Targeted expression of MYCN causes neuroblastoma in transgenic mice. EMBO J. 1997; 16:2985–95. [PubMed: 9214616]
39. Fulda S, Lutz W, Schwab M, Debatin KM. MycN sensitizes neuroblastoma cells for drug-induced apoptosis. Oncogene. 1999; 18:1479–86. [PubMed: 10050884]
40. Bordow SB, Norris MD, Haber PS, Marshall GM, Haber M. Prognostic significance of MYCN oncogene expression in childhood neuroblastoma. J Clin Oncol. 1998; 16:3286–94. [PubMed: 9779703]
41. Carr J, Bell E, Pearson AD, et al. Increased frequency of aberrations in the p53/MDM2/p14(ARF) pathway in neuroblastoma cell lines established at relapse. Cancer Res. 2006; 66:2138–45. [PubMed: 16489014]
42. Slack A, Chen Z, Tonelli R, et al. The p53 regulatory gene MDM2 is a direct transcriptional target of MYCN in neuroblastoma. Proc Natl Acad Sci. 2005; 102:731–6. [PubMed: 15644444]
43. Cheng JZ, Sharma R, Yang Y, et al. Accelerated metabolism and exclusion of 4-hydroxynonenal through induction of RLIP76 and hGST5.8 is an early adaptive response of cells to heat and oxidative stress. J Biol Chem. 2001; 276:41213–23. [PubMed: 11522795]
44. Rosse C, L'Hoste S, Offner N, Picard A, Camonis J. RLIP, an effector of the ral GTPases, is a platform for Cdk1 to phosphorylate epsin during the switch off of endocytosis in mitosis. J Biol Chem. 2003; 278:30597–604. [PubMed: 12775724]
45. Jullien-Flores V, Dorseuil O, Romero F, et al. Bridging ral GTPase to rho pathways. RLIP76, a ral effector with CDC42/Rac GTPase-activating protein activity. J Biol Chem. 1995; 270:22473–7. [PubMed: 7673236]
46. Singhal SS, Yadav S, Vatsyayan R, et al. Increased expression of cdc2 inhibits transport function of RLIP76 and promotes apoptosis. Cancer Lett. 2009; 283:152–8. [PubMed: 19375851]
47. Singhal SS, Yadav S, Drake K, Singhal J, Awasthi S. Hsf-1 and POB1 induce drug sensitivity and apoptosis by inhibiting Ralbp1. J Biol Chem. 2008; 283:19714–29. [PubMed: 18474607]
48. Singhal SS, Awasthi YC, Awasthi S. Regression of melanoma in a murine model by RLIP76 depletion. Cancer Res. 2006; 66:2354–60. [PubMed: 16489041]
49. Singhal SS, Singhal J, Yadav S, et al. Regression of lung and colon cancer xenografts by depleting or inhibiting RLIP76 (ral-binding protein 1). Cancer Res. 2007; 67:4382–9. [PubMed: 17483352]
50. Singhal SS, Singhal J, Yadav S, Sahu M, Awasthi YC, Awasthi S. RLIP76: A target for kidney cancer therapy. Cancer Res. 2009; 69:4244–51. [PubMed: 19417134]

NIH-PA Author Manuscript
NIH-PA Author Manuscript
NIH-PA Author Manuscript

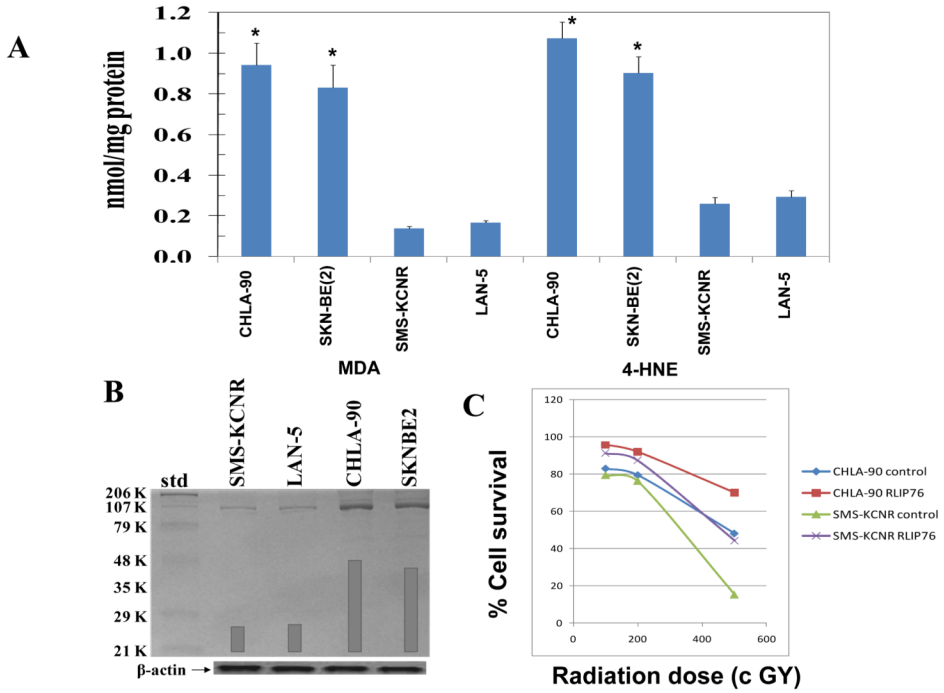

Figure 1.

Measurement of endogenous levels of 4HNE and MDA in a panel of neuroblastoma cells (**panel A**; $p < 0.001$). Expression of RLIP76 in neuroblastoma cells as assessed by Western-blot analyses using anti-RLIP76 IgG as a primary-antibodies. The bands were quantified by scanning densitometry using Innotech Alpha Imager HP. β-actin was used as a loading control (**panel B**). Protective effect of control-liposome and RLIP76-proteoliposomes (50 μg/mL) on radiation-toxicity by colony-forming assay (**panel C;** $p < 0.01$). In panels A and C, results are average and standard deviation from three separate experiments, each in triplicates ($n = 9$).

NIH-PA Author Manuscript
NIH-PA Author Manuscript
NIH-PA Author Manuscript

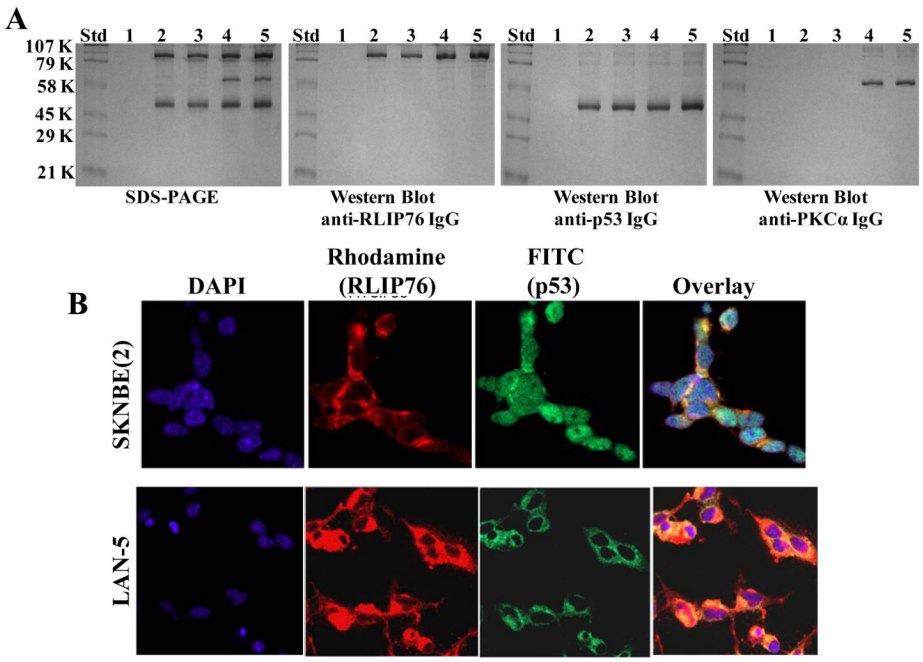

Figure 2.

Interaction of RLIP76 with p53: Purified rec-RLIP76 and p53 proteins (10 μg each), in the absence/presence of equimolar-concentration of PKCα and/or 1 mM ATP were incubated for 30 min at 37 °C and were cross-linked and immuno-precipitated as described in the methods. Cross-linked proteins were resuspended in 100 μl of SDS-PAGE sample-buffer and analyzed by SDS-PAGE, followed by Western-blots against anti-RLIP76 IgG, anti-p53 IgG, and anti-PKCα IgG. Lanes 1 to 5 shows the control with pre-immune IgG (lane 1); immuno-precipitated RLIP76 and p53 (lane 2); RLIP76, p53 and 1 mM ATP (lane 3); RLIP76, p53 and PKCα (lane 4), and RLIP76, p53, PKCα and 1 mM ATP (lane 5), respectively (**panel A**). Immuno-histochemical localization of RLIP76 and p53 in p53-mutant (SKN-BE2) and p53-normal (LAN-5) neuroblastoma cells-Red: Rhodamine for RLIP76; Green: FITC for p53, yellow overlay indicating co-localization (**panel B**).

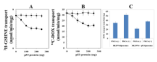

Figure 3.

Effect of p53 and PKCα on the transport-activity of RLIP76 The transport-activity of RLIP76 towards GS-HNE (**panel A**) and DOX (**panel B**) was measured by using purified rec-RLIP76 reconstituted into artificial cholesterol/asolectin liposomes as previously described (24). The effect of p53 (squares) or bovine albumin serum (round dots) at varying molar ratios was examined by incubating varying concentrations of these proteins in the transport medium. Transport medium contained RLIP76-proteoliposomes (250 ng protein/30 μL reaction-mixture), 10 μM ^{3}H-GSHNE (specific activity 3.1 × 10^{4} cpm/nmol) or 3.6 μM ^{14}C-DOX (specific activity 8.5 × 10^{4} cpm/nmol), without or with 4 mM ATP (three experiments, each in triplicate; n = 9). Heat-inactivated p53 protein was also used for additional control. The effect of p53 on PKCα-stimulated ^{14}C-DOX transport-activity of RLIP76 was also performed (**panel C**). RLIP76-liposomes alone or in combination with p53-liposomes were divided into four groups for pre-incubation for 30 min at 37 °C: (1) no ATP and no PKCα, (2) 1 mM ATP and no PKCα, (3) no ATP and 0.05 μg PKCα/μg of RLIP76, and (4) 1 mM ATP and 0.05 μg PKCα/μg of RLIP76. Transport-assay was then carried out in the established manner by addition of proteoliposomes (RLIP76 or RLIP76 + p53, 250 ng each in 30 μL reaction mixture per filtration well, in triplicates) to transport buffer containing 3.6 μM ^{14}C-DOX and either 0 or 4 mM ATP. ATP-dependent transport was calculated by subtracting uptake in the absence of ATP from that in the presence of 4 mM ATP. Results are average and standard deviation from three separate experiments, each in triplicates (n = 9).

NIH-PA Author Manuscript NIH-PA Author Manuscript NIH-PA Author Manuscript

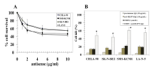

Figure 4.

Panel A: Dose-dependent cytotoxicity induced by RLIP76-antisense (R508) in neuroblastoma cells. Cells were treated with R508 using Maxfect transfection reagent (Molecula, Inc.). Cell survival was measured by MTT cytotoxicity-assay 48 h after treatment. The values are presented as mean ± SD from two separate determinations with eight replicates each (n = 16). **Panel B:** cytotoxic interactions of anti-RLIP76 IgG and CDDP. Cytotoxic effects were calculated for absorbance values obtained from MTT cytotoxicity-assays. Cells were treated alone or in combinations with anti-RLIP76 IgG (10 μg/mL) and CDDP (1 μmol/L) for 48 h before MTT assay. Eight replicates were done in three separate experiments (n = 24), *$p < 0.01$.

NIH-PA Author Manuscript
NIH-PA Author Manuscript
NIH-PA Author Manuscript

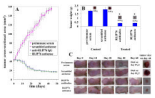

Figure 5.

Effect of anti-RLIP76 IgG and RLIP76-antisense on the size of subcutaneously implanted human Neuroblastoma cells in nude mice Twenty 11-weeks-old nu/nu mice were divided into four groups of 5 animals (treated with pre-immune serum, scrambled anti-sense DNA, anti-RLIP76 IgG, and RLIP76 antisense). All 20 animals were injected with 2×10^6 Neuroblastoma cells (SMS-KCNR) suspensions in 100 μl of PBS, subcutaneously into one flank of each nu/nu nude mouse. Animals were examined daily for signs of tumor growth. When tumors reached a cross-sectional area of ~ 40 mm^2 (~30 days later), animals were randomized treatment groups as indicated in the figure. Treatment consisted of 200 μg of RLIP76-antibodies or antisense in 100 μl PBS, i.p. Control groups were treated with 200 μg/100 μl pre-immune serum or scrambled anti-sense DNA. Tumors were measured in two dimensions using calipers. Photographs of animals were taken at day 0, day 10, day 20, day 40 and day 60 after treatment are shown for all groups. Tumor-weights and photographs of tumors were also taken at day 44 after treatment. Tumor cross-sectional area in control and experimental groups (**panels A and C**); Tumor-weight at day 44 (**panels B and C**), *$p < 0.001$, $n = 5$.

NIH-PA Author Manuscript NIH-PA Author Manuscript NIH-PA Author Manuscript

NIH-PA Author Manuscript

NIH-PA Author Manuscript

NIH-PA Author Manuscript

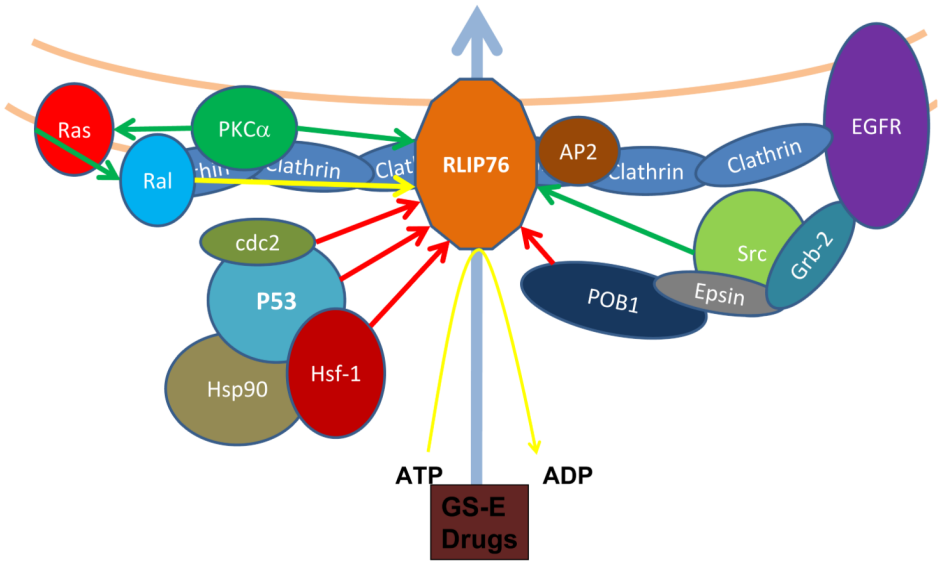

Figure 6.

RLIP76: A multi-specific regulator of multi-drug resistance and tumor-progression: RLIP76 transports the GS-E of lipid-peroxidation products and administered chemotherapy drugs out of cells, thereby reducing the cytotoxic impact of both radiotherapy and chemotherapy. In addition, RLIP76 regulates vital proliferative and metastatic signaling networks in cancer cells (Arrows: green-stimulation, red-inhibition, blue-transport and yellow-interaction). RLIP76 by its interaction with AP2 regulates the EGFR endocytosis. RLIP76 binds with CDK1 and translocates where it participates in the spindle formation during mitosis. RLIP76 is a critical mediator of PKCα-induced proliferation and drug resistance. RLIP76 enhances the migration of cells by activating GTPase R-Ras and Rac.

NIH-PA Author Manuscript

NIH-PA Author Manuscript

NIH-PA Author Manuscript

Table 1

P53 mutations and drug-resistance in neuroblastoma cell lines

Status of p53	Cell line	p53 Mutation	IC_{50} (μM)	
			DOX	CDDP
Mutated	CHLA90	E286K	0.60 ± 0.1	30 ± 4
	SK-N-BE(2)	C135F	0.88 ± 0.1	22 ± 2
Wild-type	SMS-KCNR		0.02 ± 0.0	4 ± 1
	LA –N-5		0.02 ± 0.0	10 ± 1

Drug-sensitivity assays were performed using MTT to determine IC_{50} values. The values are presented as mean ± SD from three separate determinations with eight replicates each (n = 24)